DESIGN AND IMPLEMENTATION OF GENERALIZED PROPORTIONAL INTEGRAL CONTROLLER FOR BUCK CONVERTER

L. Maheswari [1,a*], R. Sorna vadivoo[2,b], S. Vijayalakshmi[3,c]
[a,b] M.E PED (Second year), Saranathan College of Engg., Trichy, Tamilnadu, India
[c]Assistant Professor/EEE, Saranathan College of Engg., Trichy, Tamilnadu, India
[a]maheswarikrb@gmail.com, [b]sorna.r91@gmail.com ,[c]bksviji@gmail.com

Abstract:

This paper presents the GPI Controller for Buck converter. Average control signal is derived, in order to achieve the good stability of the converter and it's response is compared with the PID controller in terms of delay time 't_d', rise time 't_r', peak time 't_p', Maximum peak overshoot M_p, and settling time 't_s', to ensure the robustness of the GPI controller. In order to improve the transient response and dynamic performance of the converter, the controller parameters are designed based on the voltage mode control. The design is evaluated and verified using MATLAB/Simulink. Experimental setup has been done to evaluate the controller platform.

Key words: *Buck converter, control law, Lab view, integral reconstructor, GPI controller, PID controller.*

1. Introduction

DC power in earlier times was obtained from either the motor generator set or by converting the AC power using mercury arc rectifiers or thyratorns [1]. The obtained DC power is then converted into a variable DC power by power electronic devices known as DC-DC converter. These are having various applications such as traction motor control in electric automobile, trolley cars, marine hoist, Forklift trucks, and mine haulers. The switched mode power supplies which are used for telecommunication and computer systems requires high switching frequency, high efficiency, high power density, small size, less weight and less voltage stress. Bingol and Pacaci [2] have used a virtual laboratory, for the angular velocity task,. They have included a neural network controllers training set for a DC motor powered by a DC/DC Buck converter. The training set allows the DC motor and the controller parameters to be changed, by which the system's reaction under various operational conditions to be monitored by means of a graphical user interface. The feedback loops are designed in order to obtain the stability of the converter system. Due to some reasons like component deprivation, input voltage changes etc., the conventional designs may leads to the degradation of the closed loop performance resulting in poor dynamic stability due to change in the operating point [3-5]. This leads to the design of robust controller which achieves good dynamic performance. Among the DC-DC converters, buck converter plays a vital role in portable consumer electronics which requires only one switch and has high efficiency (90%). In this paper, a generalized proportional integral (GPI) control scheme is presented to regulate the output voltage of a "buck" converter. This control is introduced by Fliess et al. in 2002 [4]. Structural state estimators and iterated tracking error integral compensation are derived from the output feedback loop of the buck converter. Due to fast dynamic response and enhanced sturdiness with respect to unknown constant and irregular disturbances this control technique has been adopted for second order converters. GPI controllers are based on integral state reconstructors processing with the available inputs and outputs [5 - 8]. This allow regulation towards a desired output voltage for the switched-capacitor of the buck converter. The proposed GPI controller scheme is found to be robust with respect to sudden constant load variations, and it only requires the measurement of the output voltage of the inverter. Gonzalez et al. [6] have used a multivariable dc-to-dc converter, which is a boost–

boost type topology (i.e) composed of two cascaded boost converters in the continuous conduction mode. Each converter feeds an independent resistive load. A sliding-mode feedback controller, based on the GPI approach, is developed for the regulation task. The feedback control scheme uses only the output capacitor voltage measurements as well as the input signals represented by the switch positions. Mohd Tumari et al. [9], have used an H– infinity controller with pole clustering based on linear matrix inequalities techniques for controlling the velocity of a DC motor which is driven by a DC/DC Buck converter. The results were inferred, via a numerical simulations, and the proposed control scheme provide fast angular velocity tracking with minimal duty cycles. Sira-Ram ırez and Oliver-Salazar [15] presented a robust control law based on active disturbance rejection control and flatness-based control, taking into account an unknown time-varying load, for two combinations of DC/DC Buck converters and DC motors. The results of numerical simulations exhibited the robustness of the technique for the angular velocity control of the motor shaft. Many researchers have attempted to use the different controllers for various applications [9-19]. However there is no much work on experimental analysis of GPI controller using Labview. This experimental analysis using Labview provides results with a shorter duration due to its programming flexibility along with integrated tools. This method will be very useful for testing, measurements and control of DC-DC converters.

In this paper, the transient and dynamic performance of buck converter with PID and GPI controller are compared through the simulation level and the GPI controller is implemented by a computer with a data-acquisition card. This method is used for velocity control in DC motors. In order to improve the robustness of the sliding mode control, the combination of GPI and SMC controller is use for buck converter. The scheme proposes a direct regulation of the motor shaft speed using the flatness of the combined system. The paper is organized as follows: In section II, the mathematical model of the "buck" converter. Sections III and IV Modeling of buck converter with PID and GPI controller designs and its response is view through MAT lab simulink. Section V presents the comparative analysis of those converter, in terms of delay time, rise time, peak time, maximum peak overshoot and settling time. Section VI shows the experimental results of GPI controller and finally conclusion and reference are given in VII and VIII

2 Design of Buck Converter

The system of differential equations describing the dynamics of the buck converter is obtained through the direct application of Kirchhoff's current and Kirchoff's voltage law.Fig.1 shows the circuit topologies of buck converter when the position of switch is at u = 1 and u = 0. When the switch position function exhibits the value of u = 1, then the topology corresponding to the non-conducting mode of the diode is obtained. Alternatively, when the switch position exhibits the value of u = 0 then the second possible circuit topology corresponding to the conducting mode of the diode is obtained. First if the switch position function is at u = 1 and proceed to apply the Kirchoff's current and Kirchhoff's voltages laws, the resulting circuit is the one shown in Fig. 1 (a) and corresponding differential equations are

$$L\frac{di}{dt} = -v + E \tag{1}$$

$$C\frac{dv}{dt} = i - \frac{V}{R} \tag{2}$$

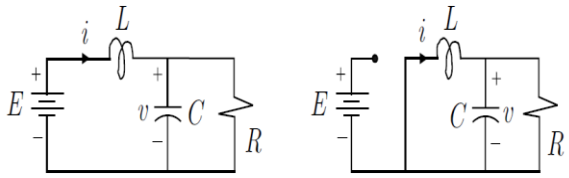

(a) switch position u=1 (b) switch Position u=0

Fig.1 Switching modes of buck converter.

when the switch position function is at u = 0 then the resulting one is similar to the Figure 1(b). Further the dynamics of the system is described by the following differential equations:

$$L\frac{di}{dt} = -v \tag{3}$$

$$C\frac{dv}{dt} = i - \frac{v}{R} \tag{4}$$

By comparing the obtained particular dynamic systems descriptions, the following unified dynamic system model can be obtained.

$$L\frac{di}{dt} = -v + uE \quad (5)$$

$$C\frac{dv}{dt} = i - \frac{v}{R} \quad (6)$$

Indeed, when u = 1 or u = 0, the Fig.1. recovers the system models (1) and (2), respectively. The Buck converter model is then represented by equation 5 and 6. In order to simplify the exposition of the model, u is replaced by u_{av}, and is used to derive the average feedback control laws, for the average (continuous) input variable u_{av}. The only feature distinguishing the average model from the switched model is the control input which will surely make the things unequal. The average model of the buck converter is described by

$$L\frac{di}{dt} = -v + u_{av}E \quad (7)$$

$$C\frac{dv}{dt} = i - \frac{v}{R} \quad (8)$$

By using state space averaging model [6], the following matrix can be obtained

$$A = \begin{bmatrix} 0 & \frac{-1}{L} \\ \frac{1}{C} & \frac{-1}{RC} \end{bmatrix} \quad (9)$$

$$B = \begin{bmatrix} \frac{u_{av}}{L} \\ 0 \end{bmatrix} \quad (10)$$

$$C = [0\ 1] \quad (11)$$

$$D = [0] \quad (12)$$

By feeding these matrices in the MATLAB simulink the transfer function can be obtained and by using this tranfer function, PID controller parameters can be determined.

3. Modeling and simulation of Buck converter with buck converter with PID and GPI Controller

A. Buck with PID Controller:

The circuit model for "buck" converter with PID controller is shown in Fig. 2. In most of the industrial applications, PID controllers are being used. The tuning parameters of this controller is obtained through the transfer function of the buck converter by using the average model of the matrix eqn. (9-12).The transfer function of the PID controller in terms of controller parameters are represented as

$$T.F_{PID}(s) = K_p\left(1 + \frac{1}{T_{i\,(s)}} + T_{d\,(s)}\right) \quad (13)$$

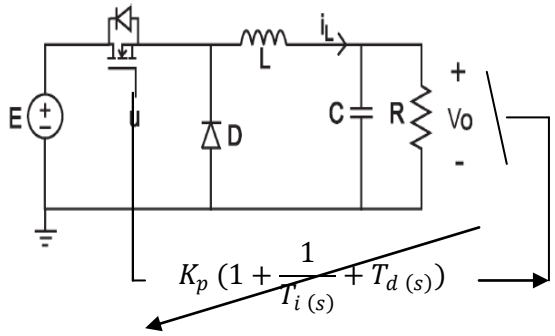

Fig. 2 Circuit model for buck converter With PID controller.

Where 'K_p' is the proportionality constant, which is proportional to the current error value, 'T_i' is the integral time constant and it is proportional to both the magnitude of the error and the duration of the error and 'T_d' is the derivative time constant and it is related to the rate of change of the process error. By "tuning" these three constants in the PID controller algorithm, the PID can provide control action designed for specific process requirements. The response of PID controller is shown in the below Fig.3.

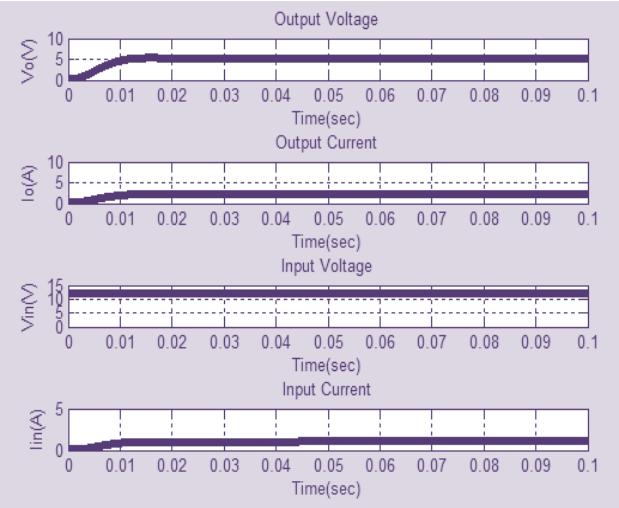

Fig. 3 Simulation result of buck with PID

B. Buck with GPI Controller:

The GPI control technique is based on integral reconstructors of the state vector. Such reconstructors obtain the state variables as a finite linear combination of iterated integrals of inputs and outputs in compliance with the system model while regarding the unknown initial conditions, and other external perturbations of classical type, as being zero. The following steps are followed to design the GPI controller. By using the average model of the matrix eqn (9-12), the Kalman controllability matrix of the system C = [b, Ab] has to be checked, which is given by

$$\frac{E^2}{L^2C} \neq 0 \qquad (14)$$

The system is controllable and hence, differentially flat. This flat output for the "buck" converter system is linear controllable and its state space form is $\dot{x} = Ax + bu$ is given by modulo a constant factor, where the linear combination of the states are obtained from the last row of the inverse of the Kalman controllability matrix.

$$F = [0,0 \ldots\ldots 1][b, Ab, \ldots\ldots, An^{-1}b]^{-1}x \qquad (15)$$

According to the preposition of the flat output, the "buck" converter is given by

$$\mathbf{F} = (\mathbf{0} \quad \mathbf{1})\begin{pmatrix} \frac{\mathbf{E}}{\mathbf{L}} & \mathbf{0} \\ \mathbf{0} & \frac{\mathbf{E}}{\mathbf{LC}} \end{pmatrix}^{-1} \begin{pmatrix} \mathbf{i_L} \\ \mathbf{v_o} \end{pmatrix}; \ F = \frac{LC}{E} v_o \qquad (16)$$

Therefore, we can simply take the output voltage variable as a flat output

$$F = v_0 \qquad (17)$$

The flatness of the system implies that all state variables of the system, including the control input variable, are parameterizable in terms of $F = v_o$ and a finite number of its time derivatives. Indeed

$$v_o = F \ ; \ i_L = C\dot{F} + \frac{1}{R}F \qquad (18)$$

and the average control input is obtained as

$$u_{av} = \frac{LC}{E}\left(\ddot{F} + \frac{1}{RC}\dot{F} + \frac{1}{LC}F\right) \qquad (19)$$

Moreover, from the average model given in eqn. (9-12), the system is also observable from the output variable Vo, i.e., the Kalman Observability matrix given by

$$O = \begin{pmatrix} C^T \\ C^T A^T \end{pmatrix} = \begin{pmatrix} 0 & 1 \\ \frac{1}{C} & -\frac{1}{RC} \end{pmatrix} \qquad (20)$$

It complies with the property of being full rank. Therefore, the system model is observable for the output $y = F = v_o$. This fact establishes the reconstructibility of the system, i.e., all of the system state variables are parameterizable in terms of the input, output and finite number of iterated integrals of the input and output variables. By integrating both sides of eqn. 19 and by solving the variable $\dot{F}$, an integral estimator of the first time derivative of F is obtained and is given as

$$\hat{\dot{F}} = \left(\frac{E}{LC}\right)\int_0^t \left[u_{av}(\tau) - \frac{1}{E}F(\tau)\right]d\tau - \frac{1}{RC}F \qquad (21)$$

$$F = v_o \qquad (22)$$

At non-zero initial states, the relations linking the actual values of the converter output voltage derivative to the structural estimate in eqns. 21 and 22 are given by

$$\dot{F} = \hat{\dot{F}} + \dot{F}_o \tag{23}$$

Where $\dot{F}_o$ denotes the unknown initial rate of change of the output voltage. The following feedback control law for the stabilization of the "buck" converter output voltage around a desired constant reference value 'F' is proposed as :

$$u_{av} = \frac{LC}{E} v + \frac{L}{ER}\dot{F} + \frac{1}{E}F \tag{24}$$

$$v = -k_3\dot{F} - k_2(F - \bar{F}) \tag{25}$$

For the GPI feedback controller, it is possible to replace the unmeasured state variable $\dot{F}$ by its structural estimated variable $\hat{\dot{F}}$ given in eqn. 22. However, this implies that the closed-loop system is affected by the constant estimation error present in $\hat{\dot{F}}$, as acknowledged in eqn. 23. To suitably correct the destabilizing effect of the structural estimation errors and the effect of possible external perturbations, GPI control uses iterated integral error compensation as follows:

$$u_{av} = \frac{LC}{E} v + \frac{L}{ER}\hat{\dot{F}} + \frac{1}{E}F \tag{26}$$

$$v = -k_3\left(\hat{\dot{F}}\right) - k_2(F - \bar{F}) - k_1\gamma - \eta k_0 \tag{27}$$

$$\dot{\gamma} = F - \bar{F} \tag{28}$$

$$\dot{\eta} = \gamma \tag{29}$$

Let e = F − $\bar{F}$ denote the stabilization error. The stabilization error dynamics is obtained by substituting (29) and controller (26-29) into the differential parameterization of the average control input given in (25). We obtain the GPI controller as follows

$$\begin{aligned} F = -k_3\left(\dot{F} - \dot{F}_0\right) - k_2(F - \bar{F}) \\ - k_1\int_0^t (F(\tau) - \bar{F})d\tau \\ - k_0\int_0^t\int_0^\tau (F(\lambda) - \bar{F})d\lambda d\tau \end{aligned} \tag{30}$$

The characteristic equation of integro-differential relation (31) in terms of the stabilization error is given by

$$e^{(4)} + K_3 e^{(3)} + K_2\ddot{e} + K_1\dot{e} + K_0 e = 0 \tag{31}$$

$$P(s) = s^4 + K_3 s^3 + K_2 s^2 + K_1 s + K_0 \tag{32}$$

The values of the design parameters $\{k_3, k_2, k_1, k_0\}$ are chosen so that the closed-loop characteristic polynomial has all of its roots in the left half of the complex plane. The controller parameters were chosen so as to achieve the following desired closed-loop characteristic polynomial:

$$P(s) = (s^2 + 2\zeta\omega_n s + \omega^2{}_n)^2 \tag{33}$$

Taking into account that ζ and ω_n are positive quantities, the gains of the GPI controller are given by

$$K_3 = 4\zeta\omega_n;\ K_2 = 4\zeta^2\omega^2{}_n;\ \ K_1 = 4\zeta\omega^3{}_n; K_0 = \omega^4{}_n. \tag{34}$$

To obtain the value of these parameter the value in equation (30) has to be substituted to get the control signal for buck converter. The simulink model is shown in fig. 4. (a) and the response of GPI controller is shown in fig. 4. (b).

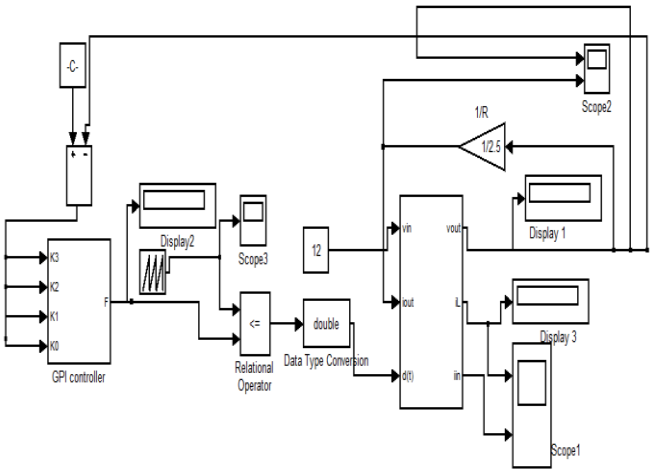

Fig. 4. (a). Simulink model of GPI controller

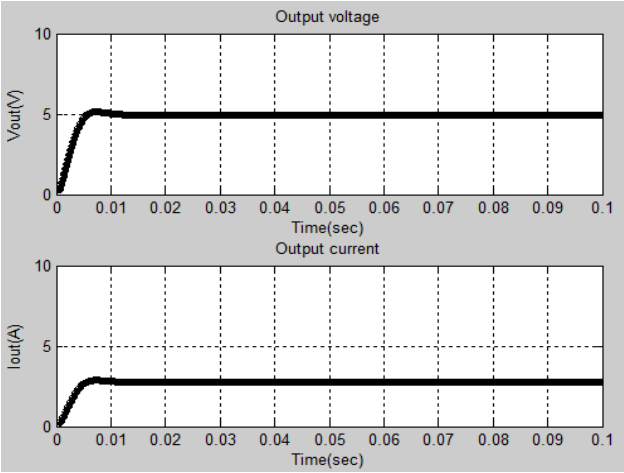

Fig. 4. (b) MAT Lab simulink model and response of Buck converter with GPI controller

4. Hardware implementation of GPI

GPI controller performance is observed through the Lab VIEW Package. It is an extensively used software for analyzing the projects experimentally with a shorter duration due to its programming flexibility along with integrated tools designed especially for testing, measurements and control. The drivers, abstraction layers and buses are provided for almost all types of instruments. The buses are used for addition, abstraction layers and drivers are provided for graphical nodes and enable to communicate effectively with the hardware devices thereby offering standard software interfaces. Front panel and functional block diagram are the main parts. The front panel shown in Fig. 5 (a) is mainly used for user interactions. The front panel opens through which inputs are passed for executing and viewing the program outputs. It provides wide varieties of small icons to perform the desired task.

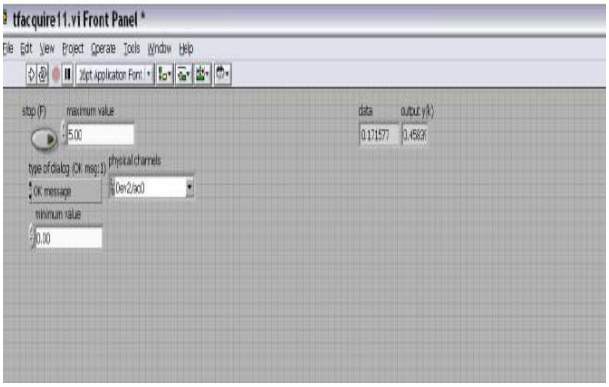

Fig. 5(a) Front Panel for GPI controller

The transfer function of the GPI controller is accessed through the front panel and corresponding functional block is given in Fig.5(b).

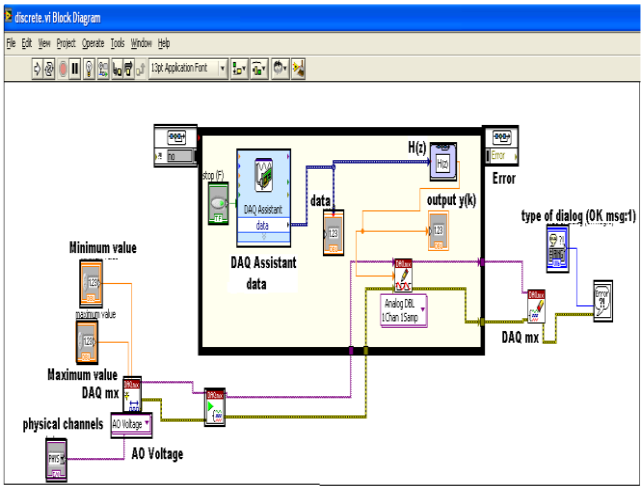

Fig. 5 (b) Functional block diagram

The block diagram, data acquisition, transfer function and signal generation are built using the functional block
diagram. The hardware implementation of GPI controller can be observed as shown in fig. 6 (a). The corresponding output response is shown in fig. 6 (b). These Lab View features makes it a superior one when compared with other development environment.

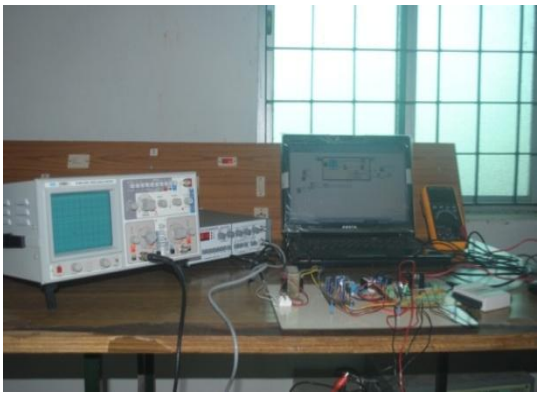

Fig .6 (a) GPI controller Setup for Buck converter

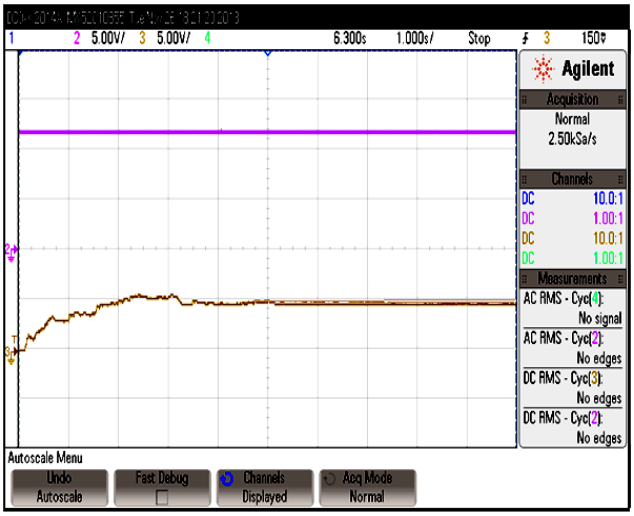

Fig .6 (b)GPI controller output

Table 1

Comparison of GPI and PID controller

Transient response Specification	**PID controller**	**GPI controller**
Delay time (t_d)	0.005s	0.002
Rise time (t_r)	0.012s	0.004
Peak time (t_p)	0.015	0.007
Maximum over shoot (M_p)	5.12%	2.1%
Settling time(t_s)	0.025	0.012
Steady state error	0.6%	.001%

The comparison of GPI and PID controller is given in table 1. The GPI controller is found to be suitable compared to PID controller.

5. Conclusion

In this paper GPI controller is implemented through Lab view software and its output is nearly equal to Matlab simulation output. From the comparative analysis, it is inferred that dynamic response of the buck converter using GPI controller gives the better response in terms of maximum overshoot, delay time, settling time and steady state error compared to PID controller. Further, it is concluded that the GPI controller has a better transient response than that achieved with a PID control action. GPI controller gives the best stabilization response. Due to which the GPI controllers are used for advanced power electronics devices, velocity control for DC motor etc.,

6. Reference

1. Ahmed M., M. Kuisma, K. Tosla, and P. Silventoinen, (2003) Implementing sliding mode control for buck converter, in Proc. IEEE PESC Rec. , vol. 2, pp. 634-637, Jun.
2. Bingol O. and Pacaci, S. (2012) A virtual laboratory for neural network controlled DC motors based on a DC-DC buck converter, Int. J. Eng. Educ , vol. 28, no. 3, pp. 713–723, 2012.
3. Edwards C. and S. K. Spurgeron, (1998) Sliding Mode Control: Theory and Applications. London, U.K.: Taylor & Francis
4. Fliess M., R. Marquez, E. Delaleau, and H. Sira-Ramírez, (2002) “Correcteurs proportionnels-intégraux généralisés,” ESAIM: Control, Optim. Calculus Variations, vol. 7, pp. 23–41
5. Forsyth A.J. and S.V. Mollow, (1998) Modeling and control of dc-dc converters, IEE power engineering journal, vol. 12, no. 5, pp. 229–236, Oct.
6. González A. F., Márquez, R. and Sira Ramírez, H. On the generalized proportional-integral sliding mode control of the boost–boost converter, in Proc. 4th ICEEE, 2007, pp. 209–212.
7. Kota Kinabalu Sabah, (2012) Proc. IEEE International Conference on Power and Energy, Malaysia, Dec. 2–5, 2012, pp.530–535.
8. Middlebrook R.D. and Cuk, S. (1976) A general unified approach to modeling switching Converter Power stages,” in Proc. IEEE PESC Rec., pp. 18–34,

9. Mohd Tumari, M. Z.. Saealal, M. S Ghazali, M. R. and Abdul Wahab, Y. (2012) H-infinity with pole placement constraint in LMI region for a buck- converter driven DC motor, in Proc. IEEE International Conference on Power and Energy, Kota Kinabalu Sabah, Malaysia, Dec. 2–5, pp.530–535.
10. Ogata, K, (1997) Modern Control Engineering. Upper Saddle River, NJ: Prentice-Hall, Inc.,
11. Rashid M. H, (2003), Power Electronics: Circuits, Devices and Applications (3rd Edition), Prentice Hall,
12. Raviraj V.S.C. and. Sen, P. C (1997) Comparative study of proportional integral, sliding mode, and fuzzy logic controllers for power converters, IEEE Trans. Ind. Appl., vol. 33, no. 2, pp. 518–524, Mar./Apr
13. Sira-Ramírez H. (2003) Sliding modes, Δ-modulators, and generalized proportional integral control of linear systems," Asian J. Control, vol. 5, no. 4, pp. 467–475, Dec.
14. Sira-Ramirez H. and Ilic, M. (1988) A geometric approach to the feedback control of switch mode DC-to-DC power supplies, IEEE Trans. Circuits Syst., vol. 35, no. 10, pp. 1291–1298, Oct..
15. Sira-Ramırez H. and Oliver-Salazar, M. A. (2013), On the robust control of Buck-converter DC-motor combinations, IEEE Trans. Power Electron., vol. 28, no. 8, pp. 3912–3922.
16. Sira-Ramírez H. and Silva-Ortigoza, R. (2006), Control Design Techniques in Power Electronics Devices. London, U.K.: Springer-Verlag
17. Sira-Ramirez, H. (2003) Sliding mode-Δ modulation control of a "buck converter", in proc. 42end IEEE Conf. Decision control, vol. 3, pp. 2999-3004, Dec
18. Venkataramanan R., (1986) Sliding Mode Control of Power Converters, PhD thesis, California Institute of Technology, California
19. Venkatramanan R., A. Sabanovic, and S. Cuk, (1985) "Sliding mode control of DC-to-DC converters," in Proc. IEEE Conf. IECON, pp. 251-258, 1985.